Opposite Changes in Work Function of Low and High Index Copper Surfaces with Surface Acoustic Wave Propagation

Hiroshi Nishiyama and Yasunobu Inoue*

Analysis Center and Department of Chemistry, Nagaoka University of Technology, Nagaoka 940-2188, Japan

Received: May 13, 2003; In Final Form: July 15, 2003

The different effects of surface acoustic waves (SAWs) on low and high index Cu surfaces were revealed by photoelectron emission microscopy (PEEM). The atomic scale surface structures of thin polycrystalline Cu films prepared by annealing and sputtering were inferred by the characteristic CO stretch frequency in the infrared reflection absorption spectra. The SAW propagation decreased the PEEM intensity for the low index planes, such as Cu(111), whereas it increased the PEEM intensity for the high index planes and step sites formed by sputtering. The results indicated that the SAWs enhanced the work function of a densely packed Cu surface and reduced that of a less packed Cu surface with coordinatively unsaturated metal atoms. Dynamic and vertical lattice displacement by SAWs was proven to have prominent effects large enough to change the electronic structures of metal surfaces.

Surface acoustic waves (SAWs) are generated on a poled ferroelectric crystal by applying rf electric power to interdigital transducer (IDT) electrodes on the crystal. We have employed SAWs to study the effects on the catalytic properties of thin polycrystalline metal (Ag, Pd, Ni) films and found that the SAWs enhanced the catalytic activities markedly for different kinds of metal-catalyzed reactions such as ethanol and CO oxidation.[1−4] Furthermore, the SAWs were useful for changing the selectivity of Cu metal-catalyzed ethanol decomposition: ethylene production increased remarkably without significant changes in acetaldehyde production.[5] King et al. investigated the SAW effects on the catalytic activity for CO oxidation of a Pt{110} film.[6−8] They also used photoelectron emission microscopy (PEEM) to examine the effects of SAWs on the adsorbed states.[9] In the presence of a $CO-O_2$ reactant mixture, the SAWs decreased the PEEM intensity of the CO-poisoned surface, indicating that the SAWs promoted CO desorption. However, in the PEEM experiments, the influences of SAWs on the geometric and electronic structures of a clean metal surface were not studied.

The enhancement of the catalytic activities and the changes in the selectivity with SAW suggest that the SAWs could affect the electronic states of the surface metal atoms. To study the SAW effects on the electronic properties of a metal surface, we have combined infrared reflection absorption spectroscopy (IRAS) with PEEM. For a polycrystalline Cu metal surface we have chosen, IRAS was used to infer the Cu surface structure on an atomic scale, whereas PEEM was employed to clarify photoemission characteristics directly related to the work function of the Cu metal while the SAW was propagating.

Figure 1a shows the structure of the sample employed. The sample was the SAW device that had two IDT electrodes on the plane of a 128°-rotated y-cut $LiNbO_3$ single crystal. The electrodes were designed to generate a wave with a wavelength of 200 μm and a frequency of 20 MHz. A polycrystalline Cu film (13×13 mm^2) was deposited at a thickness of 80 nm in the middle of the crystal surface between the two IDT electrodes, so that the SAW propagated through the Cu metal phase. The Cu film was prepared by the evaporation of Cu metal with

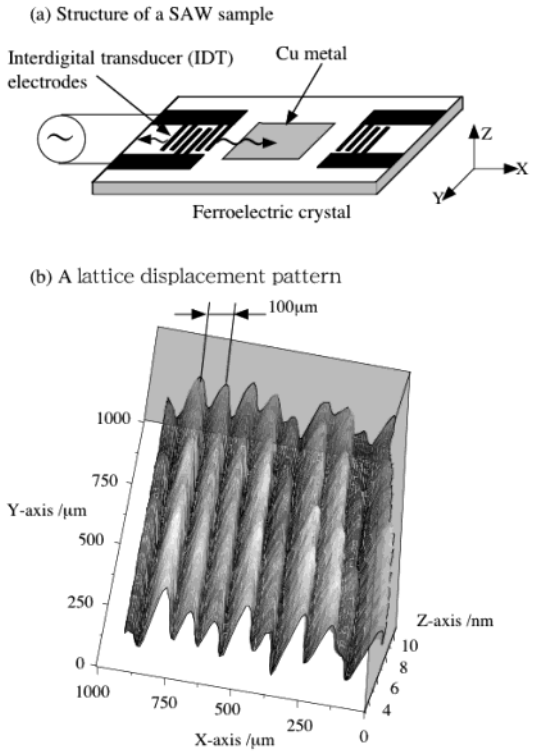

Figure 1. Schematic representation of a SAW sample with a Cu metal film (a) and three-dimensional Doppler images of the Cu surface while SAW propagates (b). SAW power: 1 W.

electron beam heating in a vacuum and by deposition at a rate of 0.5 nm s^{-1} at 473 K. After the deposition, the Cu film was either annealed at 573 K for 2.5 h under ultrahigh dynamic vacuum conditions ($<10^{-7}$ Pa) (the Cu surface was referred to as an annealed Cu surface) or sputtered at 373 K at 1000 V and then subjected to heat treatment at 573 K for 2.5 h below 10^{-7} Pa (the Cu surface was referred to as a sputtered Cu surface). Experiments were carried out using annealed and sputtered samples prepared separately and were repeated for fresh samples.

10.1021/jp035309u CCC: $25.00
Published on Web 07/31/2003

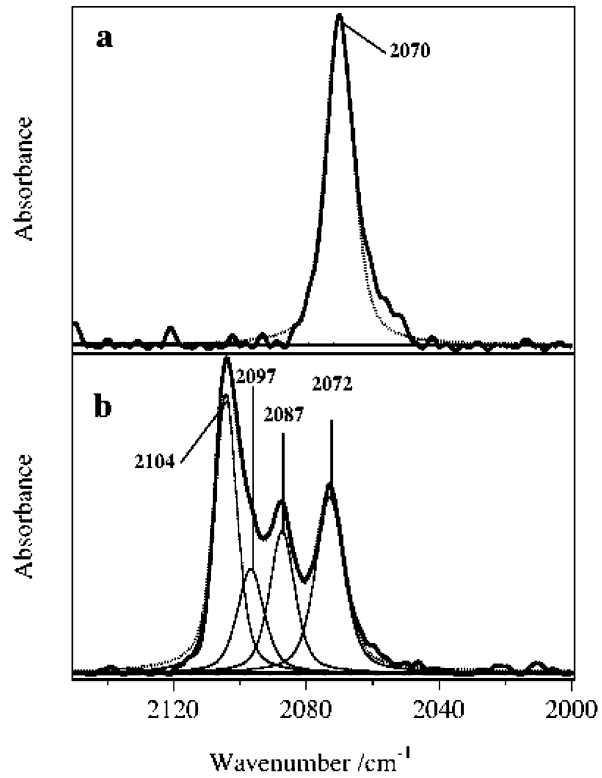

Figure 2. IRA spectra of CO adsorbed on annealed (a) and sputtered (b) Cu surfaces measured at 123 K. CO pressure: 1.3×10^{-5} Pa.

Figure 1b shows the three-dimensional Doppler images of a Cu metal surface while the SAW propagates. The images were obtained by the illumination of the Cu surface with a He−Ne laser beam and by the Doppler shift of the light beam reflected from the surface.[10] The Doppler image exhibited regular standing waves vertical to the surface, and the top-to-top distance was 100 μm. The wavelength of the SAW was calculated to be 200 μm from the finger space of the IDT. Since the top-to-top distance in the wave is given by half of a wavelength, the observed value of 100 μm is in good agreement with the calculated value. This indicates that the pattern well represents surface distortion by SAWs. The amplitude of the wave, that is, lattice displacement vertical to the Cu surface, reached 11 nm at a rf power of 1.0 W. The effects of lattice displacement on the surface atom distance were estimated by taking the ratio of amplitude to wavelength into account. By the assumption of uniform linear elongation by the wave, changes in atom−atom distance at the surface were calculated to be on the order of 10^{-5}%.

IRAS can be used to infer the atom scale differences in the structure of polycrystalline metal surfaces prepared by annealing and sputtering. When the absorption frequencies of an adsorbate on different crystal faces are available, frequently, CO is used as a probe molecule, and the vibration frequencies of the adsorbed CO offer information on the structure of Cu surfaces. Figure 2a shows an IRA spectrum of CO adsorbed at a pressure of 1.3×10^{-5} Pa at 123 K on an annealed Cu surface. Only a symmetric single peak was observed at 2070 cm^{-1}. Figure 2b shows the spectrum of CO adsorbed on a sputtered Cu surface under the same adsorption conditions. The Cu surface provided a broad spectrum with three major peaks. The deconvolution showed that the complex spectrum could be divided into four peaks appearing at 2072, 2087, 2097, and 2104 cm^{-1}. The IRAS study of CO adsorption on Cu single crystals showed that the CO stretch frequency appeared at 2070 cm^{-1} on Cu(111),[11,12]

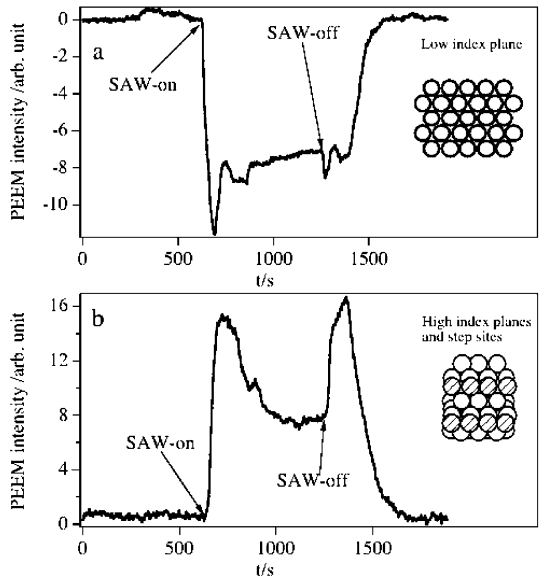

Figure 3. Opposite changes in the PEEM intensity between annealed (a) and sputtered (b) Cu surfaces with SAW propagation. Circles with slanted lines in them represent coordinatively unsaturated surface atoms. Measurements are at room temperature under UHV conditions ($<5 \times 10^{-8}$ Pa).

2087 cm^{-1} on Cu(100),[11,13,14] and 2093 cm^{-1} on Cu(110)[15,16] at a saturation coverage of CO. On the other hand, for CO adsorption on the high index planes, a symmetric narrow band center was observed at 2110 cm^{-1} on Cu(211), 2104 cm^{-1} on Cu(311), and 2106 cm^{-1} Cu(755) for saturation coverage.[17] For CO adsorbed on Cu particles supported on SiO_2,[18] a frequency band of 2074 cm^{-1} was assigned to a Cu(111)-like structure, the 2094 cm^{-1} band to a (110)-like structure, and the 2087 cm^{-1} band to a (100)-like structure. In addition, the 2108−2110 cm^{-1} band was associated with structures related to the high index planes such as (211) and (311). Furthermore, for the evaporated Cu films that had a large density of step sites, CO adsorption exhibited a band at 2102 cm^{-1} at saturation coverage.[19]

From the comparison of the CO stretch frequencies, a single peak at a frequency of 2070 cm^{-1} for the annealed Cu surface can be assigned to the stretch frequency of CO adsorbed on Cu(111), which is the thermodynamically most stable surface. On the other hand, for the sputtered Cu surface, the three absorption bands 2072, 2087, and 2097 cm^{-1} are close to those of CO stretch frequencies adsorbed on the (111), (100), and (110) planes, respectively, whereas the large 2104 cm^{-1} band is assigned to the frequency of CO on the high index planes such as the (311) and (755) planes and step sites. From the IR spectra for CO adsorbed, therefore, it is evident that the annealed Cu surface mainly consists of a low index plane such as Cu(111), whereas the sputtered Cu surface exposes a high density of the high index planes and step sites.

PEEM provides a magnified image of the surface due to contrasts in intensity of photoelectrons emitted from the surfaces irradiated by UV light.[20] Figure 3 shows changes in the PEEM intensity with SAW-on and -off under ultrahigh vacuum conditions. When the SAW propagated on the low index Cu(111) plane of the annealed Cu surface, the PEEM intensity decreased sharply. After partial recovery, the intensity reached a stationary level. With SAW-off, after small fluctuations, the intensity returned to the original zero level. On the other hand, for the high index planes and step sites of the sputtered Cu surface, the SAW-on gave rise to a sharp increase in the PEEM intensity, followed by a gradual decrease. After a broad transient

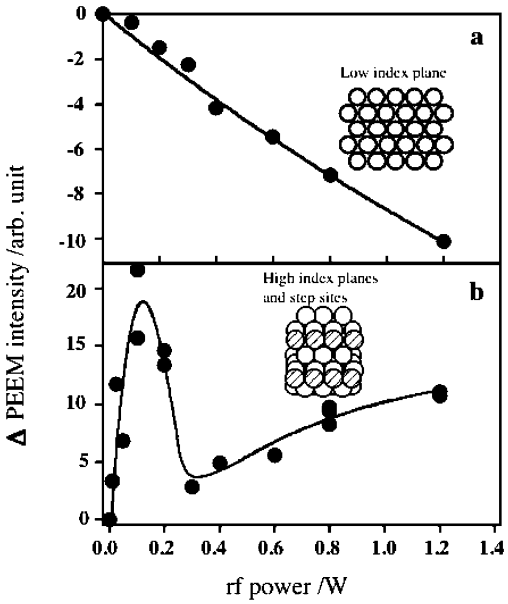

Figure 4. Changes in the PEEM intensity of annealed (a) and sputtered (b) Cu surfaces with increasing SAW power. Circles with slanted lines in them represent coordinatively unsaturated surface atoms.

change, the intensity reached a constant level. With SAW-off, the PEEM intensity increased once and rapidly decreased to the zero level. The PEEM intensity changes were reversible with the SAW-on and SAW-off.

Figure 4 shows the PEEM intensity as a function of SAW power. For the low index Cu(111) plane, the PEEM intensity decreased monotonically with increasing SAW power. For the high index planes and step sites, the PEEM intensity increased with increasing power, passed through a maximum, decreased sharply, and increased gradually.

A PEEM image reflects the work function changes in the observed field. From the PEEM intensity behavior, it is apparent that the SAW increased the work function of the low index Cu (111) surface, whereas it decreased that of the high index planes and step sites. Interestingly, a decrease in the work function for the rough Cu surface with SAW-on was opposite to the enhancement of the work function for the smooth Cu surface.

A model for the work function of a metal surface shows that free electrons spill out toward vacuum (just outside) from the topmost surface, and an electric double layer is formed by a pair of the "spill out" electrons and positive charges remaining just inside the metal.[21,22] The potential barrier of the layer is related to the work function of the metal. The dependence of the work function on the crystallographic orientations is attributed to the differences in the density of "spill out" electrons among the crystal faces: the work function of a closely packed smooth Cu surface is larger than that of a surface that is rougher on an atomic scale (a less packed surface), as demonstrated by the fact that the work function of Cu metal is 4.94 eV for Cu-(111), 4.59 eV for Cu(100), and 4.48 eV for Cu(110).[23] The opposite changes in the work function in the presence of the SAW between the low and high index Cu surfaces are explained in terms of atomic scale structure differences of the surfaces. For the low index Cu(111) surface, it is difficult for the SAW to affect the atom−atom distance and arrangements sufficiently, because of the closely packed geometry. However, the dynamic and vertical lattice displacement due to SAW is likely to have enhancing effects on the extent of electrons that spill out from the surface, because the direction of the movement of lattice displacement is the same as the direction in which electrons

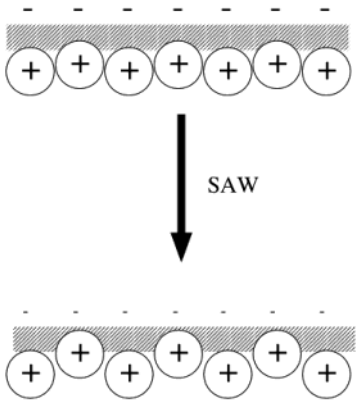

Figure 5. Schematic representation of a model for work function decreases in high index planes by SAWs. Coordinatively unsaturated surface atoms stick out in the presence of SAWs, and protruding, positively charged Cu cores reduce the electric double layer (dipole moment).

spill out. This leads to the formation of a larger electric double layer and hence to the increases in the work function. Similar changes occur for the high index and step sites. However, a large difference in the high index planes and step sites is the presence of a high density of coordinatively unsaturated Cu surface atoms. It is likely that the surface atoms are largely influenced by lattice displacement induced by SAWs, since they are loosely bound, and lattice distortion is known to be significantly concentrated on unsaturated and irregular sites such as dislocations and vacancies.[24] It would be possible that the SAW permits the unsaturated Cu ion cores to stick out into the electric double layer. Protruding Cu atoms reduce the electric double layer, because of rougher Cu surfaces on an atomic scale at the sites, as schematically represented in Figure 5. This apparently leads to decreases in the work function. Namely, work function decreases in the high index planes and step sites with SAW propagation are associated with atomic scale geometry changes in the coordinatively unsaturated surface atoms. At the present time, it seems difficult to explain the complicated behavior in the PEEM intensity with increasing SAW power (Figure 4). A possible explanation for the decreasing portion, however, is that an increase in rf power enhances the density of "spill out" electrons at the sites in a fashion similar to that observed for the low index Cu surface. In other words, as the contribution of an electric double layer becomes significant with increasing rf power, the PEEM intensity tends to decrease.

The present PEEM and IRAS study clearly demonstrated that SAWs caused opposite work function changes with smooth and rough Cu surfaces. It is quite surprising to see that a small dynamic and vertical lattice displacement of the SAW has marked influences on the structures of Cu surfaces to the extent to which the photoemission behavior varies. Although we need to examine whether effects are unique for Cu metal or generic for metals, the present findings are encouraging for the development of a physical method to artificially change the work function of metal surfaces by dynamic and vertical lattice displacement.

Acknowledgment. We thank Dr. N. Saito for his assistance in Doppler shift measurements. This work was supported by a grant-in-aid for Scientific Research A (15206088) from The Ministry of Education, Science, Sports and Culture.

References and Notes

(1) Inoue, Y.; Matsukawa, M.; Sato, K. *J. Am. Chem. Soc.* **1989**, *111*, 8965.

(2) Inoue, Y.; Matsukawa, M.; Sato, K. *J. Phys. Chem.* **1992**, *96*, 2222.
(3) Inoue, Y.; Matsukawa, M.; Kawaguchi, H. *J. Chem. Soc., Faraday Trans.* **1992**, *88*, 2923.
(4) Nishiyama, H.; Saito, N.; Yashima, M.; Watanabe, Y.; Inoue, Y. *Faraday Discuss.* **1997**, *107*, 425.
(5) Nishiyama, H.; Saito, N.; Yashima, T.; Sato, K.; Inoue, Y. *Surf. Sci.* **1999**, *427*/*428*, 152.
(6) Kelling, S.; Mitrelias, T.; Matusmoto, Y.; Ostanin, V. P.; King, D. A. *Faraday Discuss.* **1997**, *107*, 435.
(7) Kelling, S.; Mitrelias, T.; Matusmoto, Y.; Ostanin, V. P.; King, D. A. *J. Chem. Phys.* **1997**, *107*, 5609.
(8) Mitrelias, T.; Kelling, S.; Kvon, R. I.; Ostanin, V. P.; King, D. A. *Surf. Sci.* **1998**, *417*, 97.
(9) Kelling, S.; Cerasari, S.; Rotermund, H. H.; Ertl, G.; King, D. A. *Chem. Phys. Lett.* **1998**, *293*, 325.
(10) Saito, N.; Nishiyama, H.; Sato, K.; Inoue, Y. *Chem. Phys. Lett.* **1998**, *297*, 72.
(11) Chesters, M. A.; Parker, S. F.; Raval, R. *Surf. Sci.* **1986**, *165*, 179.
(12) Hayden, B. E.; Kretzschmar, K.; Bradshaw, A. *Surf. Sci.* **1985**, *155*, 553.
(13) Ryberg, R. *Surf. Sci.* **1982**, *114*, 627.
(14) Horn, K.; Pritchard, J. *Surf. Sci.* **1976**, *55*, 701.
(15) Hollins, P.; Davies, K. J.; Pritchard, J. *Surf. Sci.* **1984**, *138*, 75.
(16) Horn, K.; Hussain, M.; Pritchard, J. *Surf. Sci.* **1977**, *63*, 244.
(17) Pritchard, J.; Catterick, T.; Gupta, R. K. *Surf. Sci.* **1975**, *76*, 1.
(18) Xu, X.; Goodman, D. W. *J. Phys. Chem.* **1993**, *97*, 683.
(19) Dumas, P.; Tobin, R. G.; Richards, P. L. *Surf. Sci.* **1986**, *171*, 579.
(20) Engel, W.; Kordesch, M. E.; Rotermund, H. H.; Kubala, S.; von Oertzen, A. *Ultramicroscopy* **1991**, *36*, 148.
(21) Lang, N. D.; Kohn, W. *Phys. Rev. B* **1971**, *3*, 1215; *Phys. Rev. B* **1970**, *1*, 4555.
(22) Skriver, H. L.; Rosengaard, N. M. *Phys. Rev. B* **1992**, *46*, 7157.
(23) Gartland, P. O.; Berge, S.; Slagsvold, B. *J. Phys. Rev. Lett.* **1972**, *1*, 738.
(24) Kittel, C. *Introduction to Solid State Physics*, 7th ed.; John Wiley & Sons: New York, 1996; p 590.